Mining of Mineral Deposits
Volume 19 (2025), Issue 4, 22-30

MMD JOURNAL / MINING.IN.UA

https://doi.org/10.33271/mining19.04.022

Using a combined electromagnetic conversion method to determine iron ore characteristics

Volodymyr Morkun [1], Natalia Morkun [1], Tetiana Oliinyk [2], Svitlana Hryshchenko [3*]

[1] *Bayreuth University, Bayreuth, Germany*
[2] *Kryvyi Rih National University, Kryvyi Rih, Ukraine*
[3] *State Tax University, Irpin, Ukraine*

**Corresponding author: e-mail smgrischenko@gmail.com*

Abstract

Purpose. Determination of characteristic parameters of electromagnetic eddy current conversion for the recognition of mineralogical varieties of iron ore.

Methods. The work uses methods of analysis of domestic and foreign experience, mathematical analysis, and computer modeling to determine the influence of specific physicochemical properties and textural and structural features of iron-bearing rocks on the characteristics of eddy current conversion of a probing electromagnetic signal. To determine the frequency of the probing signal at which the real and imaginary components of the impedance of the sensor's measuring coil are equal to each other, it is approximated using a Foster network.

Findings. Variations in the electrical conductivity and magnetic permeability of iron ore, associated with its mineralogical composition and physical structure, lead to changes in the conditions of formation and flow of eddy currents, which is reflected in the phase, amplitude, and spectral composition of the signal in the receiving circuit of the eddy current sensor. The measured impedance values of the sensor's measuring coil characterize the unique properties of the rock sample under study and, together with the frequency value of the probing electromagnetic signal, are a characteristic feature of the mineralogical variety of rock.

Originality. It has been established for the first time that the values of the real and imaginary components of the impedance of the measuring coil and the frequency at which they are equal to each other, determined by the results of eddy current conversion in a ferromagnetic medium of a probing electromagnetic signal of variable frequency, correspond to the unique physicochemical properties of the mineralogical varieties of the iron-bearing rock under study and are effective characteristic features for their recognition.

Practical implications. The dependencies obtained as a result of modeling eddy current conversion are used in the implementation of the method of non-contact non-destructive measurement of iron ore characteristics and recognition of its mineralogical varieties. The results of testing and practical application of the proposed method demonstrate its high efficiency, which allows us to recommend the developed scientific and technical solutions for wide industrial application in mining enterprises.

Keywords: *eddy current transformation, rock modeling, characterization, measurement of characteristics*

1. Introduction

Exploration and mining operations must be carried out in such a way as to ensure the systematic development of mineral deposits, their efficient use, and the protection of the environment. An important element of this process is the rapid determination of the physical, mechanical, chemical, and mineralogical characteristics of the extracted raw materials. Non-destructive, non-contact testing methods are the preferred approach to solving this problem. The physical effects associated with the electromagnetic eddy current conversion procedure can be used to determine the characteristics of iron ore at all stages of its deposit development.

In eddy current nondestructive testing, an alternating current excitation coil induces an eddy current in the sample by means of electromagnetic coupling. In turn, the circulation of the eddy current induces a secondary magnetic field. This field changes with changes in the electrical conductivity, magnetic permeability, and structural features of the sample. The change in field is picked up by a sensing device, which is usually a coil or magnetic sensor. Eddy current measurements do not require surface preparation of the controlled sample, which leads to shorter inspection times and increased process efficiency. Eddy current systems are relatively economical and reliable [1]. At the same time, the use of eddy current systems to assess the characteristics of rock requires substantiation of their design, parameters, and functioning algorithms. The eddy current non-destructive testing (ECT) method is widely used in industrial enterprises to determine physical and geometric properties, as well as to diagnose electrically conductive structures [2], [3]. Measuring the thickness of metal materials using the ECT method has become very attractive in the last few years [4]. The flow of

Received: 15 April 2025. Accepted: 23 October 2025. Available online: 30 December 2025

Mining of Mineral Deposits. ISSN 2415-3443 (Online) | ISSN 2415-3435 (Print)

eddy currents in a conductive material depends on many parameters, such as the frequency of the applied sinusoidal current, the physical and geometric properties of the material, and the so-called standard penetration depth [5], [6]. This last parameter represents the time-varying concentration trend of the induced current near the material surface. For homogeneous and isotropic materials, an increase in the operating frequency leads to an increase in the current concentration near the surface and a concomitant increase in resistance and decrease in inductance of the excitation coil [7].

Decisions on sensor design are often related to the number of coils, materials used, and compensation measures for the implementation of measurements. Paper [8] presents a single-coil system for large displacement ranges in environments with high temperatures and significant fluctuations. The approach is based on a sensor design derived from an equivalent circuit model (ECM). The proposed single-coil sensor design maintains a position error of less than 0.2% of the full scale when the temperature changes in the range of 100-110 K. Eddy current sensors are resistant to aggressive environments such as dirt, dust, and moisture [9]. Their non-contact and compact design makes them affordable and widely used [10].

In the practice of determining the geophysical properties of rocks, the results of measuring their resistivity and magnetism are widely used. Measurements are performed in borehole and on core samples in the laboratory to obtain information on physical properties for the evaluation of ground-based geophysical prospecting methods. Down hole measurements are valuable as a complement to regular core analysis and description [11].

Paper [12] proposes a combined method for determining the characteristics of rocks based on the use of both electromagnetic acoustic and eddy current transformations. As a result of the electromagnetic acoustic transformation, ultrasonic waves are generated in the medium under study, the propagation process of which is the subject of further analysis.

Works [13], [14] consider the theoretical foundations and practical results of using ultrasonic measurements of the physical, mechanical, chemical, and mineralogical characteristics of ore raw materials and its processed products. The electromagnetic properties of rocks are also the physical basis of eddy-current transformation, so the use of a method of controlling rock characteristics based on this phenomenon can help to improve the results obtained with minimal additional costs [15].

At the same time, it should be noted that the specific physicochemical properties and textural and structural features of iron-bearing rocks require additional research to determine the characteristic parameters of the measured signals for high-quality recognition of mineralogical ore varieties.

The objective of the study is to substantiate the use of eddy current transformation to determine the characteristics of iron ore raw materials using the analysis of domestic and foreign experience, methods of mathematical and simulation modeling of the eddy current measurement procedure.

2. Methods

The physical and geological model (PGM) of an iron ore deposit is formed on the basis of a schematic geological section and astrophysical data. The FGM is a section with formalized boundaries and physical properties of all the represented rock types. These properties of the objects in the emerging FGM are determined using all available types of measurements and analysis of the results.

To evaluate the characteristics of iron-bearing rocks with electrical conductivity and magnetic permeability, the eddy current testing (ECT) method can be used.

ECT eddy current testing is based on electromagnetic induction. An alternating current in the excitation coil *1*, which is placed next to the test medium *2*, creates an alternating magnetic field *3*, which forms eddy currents *4* in it (Fig. 1) [13], [16]. Eddy currents induce a secondary magnetic field *5*. The parameters 6 of these processes are measured using the second (receiving) coil or by measuring the parameters of the current flowing in the excitation coil *1*.

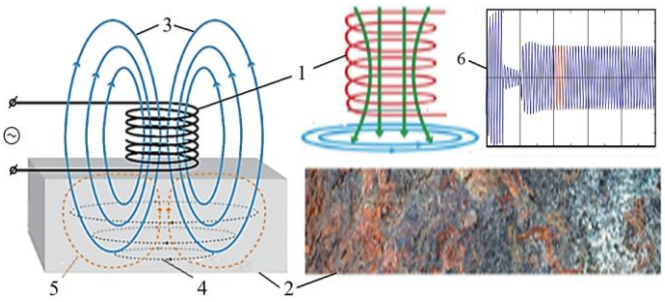

Figure 1. Basic principles of eddy current measurements: 1 – the excitation coil; 2 – the test medium; 3 – magnetic field; 4 – eddy currents; 5 – eddy currents generate a secondary field; 6 – the resulting signal for detecting structural or surface changes

Variations in the electrical conductivity and magnetic permeability of the object under control, in particular iron-bearing rocks, associated with their specific physical and chemical properties and textural and structural features, lead to changes in the conditions of formation and flow of eddy currents, which affects the phase, amplitude and spectral composition of the signal in the receiving circuit.

The electromagnetic properties of rocks vary widely. Information on the electrical resistance of materials given in different sources often differs significantly. This is explained by both the methods of their determination and the degree of purity, as well as the difference in structure, hygroscopic, humidity, and temperature of the samples under test.

It is stated in [11] that the resistivity of iron-bearing rocks varies widely and usually depends on the porosity of the rock and the type of ferrous material in it. Rocks containing iron carbonate and iron silicate minerals have a high resistivity (400 to 1000 ohms), while most rocks containing secondary hematite have a moderately low resistivity (20 to 100 ohms) due to their higher porosity. Siliceous, magnetite, and specula rite-containing taconites have extremely low resistivity (less than one ohm-m) due to electrical conductivity through the metallic mineral grains rather than through pore water. Associated silicate-magnetite rocks have high resistivity (500 to 1000 ohms). In general, the rocks adjacent to the iron formation have a much higher resistivity (1000 to 5000 ohms) than the rocks of the iron formation. Measurements of magnetic susceptibility in boreholes and in the laboratory have not revealed a direct relationship between magnetite content and resistivity [11].

Table 1 shows the average values of magnetic susceptibility, and Table 2 shows the electrical conductivity and dielectric constant of some minerals.

Table 1. Magnetic susceptibility of minerals

Minerals	Chemical formula	Magnetic susceptibility, SI
Magnetite	Fe_3O_4	8.8-25.0
Magnetite	γFe_2O_3	3.8-25.0
Titanium magnetite	$Fe(Fe^{3+}, Ti)_2O_4$	10^{-S}-1
Pyrothin	$Fe_{1-x}S$ (x = 0.1-0.2) $Fe_{1-x}S$ (x = 0.1-0.2)	0.13-1.3
Hematite	Fe_2O_3	$(1.3\text{-}13.0)\cdot10^{-3}$
Siderite	$FeCO_3$	$(2.7\text{-}7.5)\cdot10^{-3}$
Goethite	αFeOOH	$(2.5)\cdot10^{-4}$
Jacobsit	$MnFe_2O_4$	250
Trevolit	$NiFe_2O_4$	6.3

Table 2. Electrical properties of minerals

Minerals	Dielectric constant	Specific electrical conductivity, S/m
Magnetite	33.7-81	10000-0.01
Hematite	25	100-0.01
Siderite	5.2	10-0.0001
Ilmenite	33.7-81	10000-100
Pyrolusite	> 81	10000-10

The concentration of the induced eddy current near the surface of the conductive material under investigation is associated with the skin effect phenomenon.

The penetration of the eddy current into the sample material is limited due to the skin effect, which causes its density to decrease exponentially with depth. Eddy current density J_x (x – component) decreases in the z direction according to the Expression [5]:

$$J_x(z) = J_x(0)e^{kz}e^{-jkz}, \quad (1)$$

where:

$J_x(0)$ – density of eddy currents on the surface of the conductive material (z = 0).

$$k = \sqrt{\frac{\mu\sigma w}{2}}, \quad (2)$$

where:

ω – corner frequency, rad/s;

μ – magnetic permeability, H/m;

σ – electrical conductivity, S/m.

The amplitude of the eddy current density decreases in (1/e) times compared to its surface amplitude at a distance δ:

$$\delta = \sqrt{\frac{2}{\mu\sigma w}}, \quad (3)$$

where:

δ – skin layer thickness, m.

Equation (3) shows that the penetration depth depends on the excitation frequency. The lower the frequency, the deeper the penetration, and vice versa.

The excitation in the rock and the determination of the parameters of the probing electromagnetic signal are carried out using a measuring coil K_1, located in proximity to the rock surface. The measuring coil K_1 is wound with n turns of wire and is supplied with a measuring signal of a certain amplitude (voltage U) and frequency f. At the same time, an alternating current flows in it:

$$I = I_0 cos(wt), \quad (4)$$

where:

$w = 2\pi f$;

f – current frequency;

I_0 – amplitude;

t – time.

The material under study (rock) can be represented as a virtual coil with an air core K_2 [5], [17], [18]. When next to the measuring coil K_1 no test medium, its impedance Z_0 is a complex value:

$$Z_0 = R_0 + jX_0, \quad (5)$$

where:

R_0, jX_0 – real and imaginary parts Z_0.

Value $X_0 = 2\pi f L_0$ proportional to frequency f and inductance of the measuring coil L_0.

When the measuring coil K_1, energized equipment U, approaches the environment under study, in it, i.e. in a virtual coil K_2, eddy currents occur I_e. Eddy currents create a secondary magnetic field that interacts with the primary field. As a result, the new impedance of the measuring coil K_1 is equal to Z_c:

$$Z_c = R_c + jX_c, \quad (6)$$

where:

R_c, jX_c – represent the real and imaginary parts Z_c.

In this case, the imaginary part Z_c is defined by the expression $X_c = 2\pi f L_c$.

Impedance Z_c depends on the characteristics of the sensor coil, operating frequency f, properties of the test medium and measurement geometry x:

$$Z_c = \left[R_0 + R_e(x,\sigma,\mu,f)\right] + jw\left[L_0 - L_e(x,\sigma,\mu,f)\right], \quad (7)$$

where:

R_0, L_0 – resistance and inductance of the measuring coil K_1 when there is no test medium nearby;

R_e, L_e – resistance and inductance caused by eddy current;

σ – electrical conductivity of the test medium;

μ – magnetic permeability of the test medium.

The relationship between the measuring coil K_1 and the environment under study, i.e., a virtual coil K_2, can be represented as a weakly coupled transformer with an air core [19], [20].

The primary circuit of the transformer (measuring coil K_1) is a series-connected resistor R_0 and an inductor coil L_0. The secondary (shorted) winding of the transformer (the medium under study, i.e., the virtual coil K_2) is also represented by a series-connected resistor R_t and an inductor coil L_t. According to Kirchhoff's law, this structure is defined by the following system of equations [21]:

$$R_o I + jwL_0 I - jwMI_e = U; \quad (8)$$

$$R_t I_e + jwL_t I_e - jwMI = 0, \quad (9)$$

where:

$w = 2\pi f$;

R_o that L_o – resistance and inductance of the measuring coil K_1, when there is no research environment nearby;

R_1 that L_1 – accordingly, the resistance and inductance of the virtual coil K_1;

M – mutual inductance between two coils.

The value of R_t is determined by the resistance of the circuit in which eddy currents flow, i.e., the resistance R_t is proportional to the specific resistance of the medium under study. When there is no medium under study near the sensor, the measured total resistance of the primary circuit is equal to

Z_o. As the sensor approaches the conductive medium under study, the complex resistance of the primary circuit becomes equal to Z_c:

$$Z_c = \left[R_0 + \mathrm{R_e}(x)\right] + jw\left[L_0 - L_e(x)\right] = R_c(x) + jwL_c(x), \quad (10)$$

By solving the system of Equations (8) and (9), we can obtain:

$$L_c = L_0 - \frac{w^2M^2}{R_t^2 + (wL_t)^2} L_t = L_0 - L_e, \quad (11)$$

$$R_c = R_0 + \frac{w^2M^2}{R_t^2 + (wL_t)^2} R_t = R_0 + R_e, \quad (12)$$

where:

M – the mutual inductance between the coil and the medium under study, determined by the expression:

$$M = k(x)\sqrt{L_c L_t} \quad (0 < k < 1), \quad (13)$$

where:

k – coupling coefficient between the primary and secondary windings of the transformer, which depends on the geometry of the measurements x.

Taking into account (10), (11), and (12), we obtain:

$$Z_c = \left[R_0 + \frac{w^2M^2}{R_t^2 + (wL_t)^2} R_t\right] + jw\left[L_0 - \frac{w^2M^2}{R_t^2 + (wL_t)^2} L_t\right]. \quad (14)$$

Thus, the measured impedance, equivalent resistance (the real part of the impedance), and inductance (the imaginary part of the impedance) depend on the properties of the medium under study and are characteristic features of mineralogical rock types. As follows from expression (7), each of the above parameters has a multifunctional dependence on the characteristics of the medium under study (σ – electrical conductivity, μ – magnetic permeability), and the frequency of the probing signal f and measurement geometry x.

In order to determine the main factors affecting the impedance of the sensor coil when it is located near an iron-bearing rock, we simulated this scenario in Matlab 2021b using the Eddy Current Scenario Simulator software package [22]. Using this software package, a scenario was considered when the coil is located above the conducting half-space at a distance of L_0 (Fig. 2).

Half-space, i.e. rock, is characterized by electrical conductivity σ and magnetic permeability μ_r. These parameters, as well as the coil parameters (outer radius r_0, inner radius r_i, coil height l and the number of turns n) are used to generate the corresponding dependencies on the impedance plane. The current in the coil that creates the primary magnetic field has a frequency of f.

The intrinsic impedance of the sensor coil is calculated according to the Expression [22]:

$$Z_0 = j2w\pi\mu_0 v^2 \int_0^\infty \frac{\aleph^2(kr_i, kr_0)}{k^6}\left(e^{-kl} - 1 + kl\right)dk; \quad (15)$$

$$v = \frac{n}{(r_0 - r_i)\cdot l}. \quad (16)$$

When implementing this calculation, numerical integration is performed using the function Matlab in the range from 0 to k_{max}.

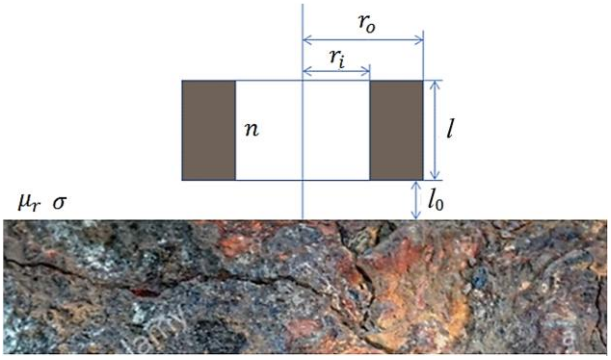

Figure 2. Schematic of the eddy current control model: σ – electrical conductivity; μr – magnetic permeability; r0 – outer radius; ri – inner radius; l – coil height; n – the number of turns; f – frequency

To determine the change in the coil impedance due to the presence of a half-space of the material under study, the Formula is used [22]:

$$Z = jw\pi\mu_0 v^2 \int_0^\infty \frac{\aleph^2(kr_i, kr_0)}{k^6} \cdot \left\{2\left(e^{-kl} - 1 + kl\right) - \frac{\mu_r k - y}{\mu_r k + y} \times \left[e^{-2kl_0} + e^{-2k(1+l_0)} - 2e^{-k(1+2l_0)}\right]\right\} dk. \quad (17)$$

Thus, Expression (15) defines the reactance of an isolated coil, and Expression (17) defines the unnormalized impedance of the coil in the presence of the medium under study.

The impedance measurement procedure was modeled using the Simscape® extension for Simulink® /MATLAB® [23]. Figure 3 shows a diagram of the model.

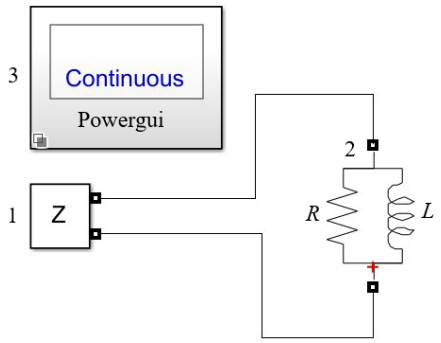

Figure 3. Scheme of the model for measuring the parameters of electromagnetic eddy current conversion

The following blocks are used in this model: the Impedance Measurement block from the Simscape / Electrical / Specialized Power Systems / Sensors and Measurements library; the Parallel RLC Branch block from the Simscape / Electrical / Specialized Power Systems / Passives library; and the Powergui block from the Simscape / Electrical / Specialized Power Systems library.

The Parallel RLC Branch block implements a resistor, an inductor, and a capacitor or their parallel combination. In the circuit shown in Figure 3, the parasitic capacitance of the electrical circuit is not taken into account, so there is no capacitor.

The impedance measurement unit measures the impedance between two nodes in a linear circuit as a function of frequency. It consists of a current source I_z, connected between the inputs of the impedance measurement unit and the voltage meter U, connected through the terminals of the

current source. The network impedance is calculated as a function of the transmission $H(s)$ from the input current to the output voltage of the state space model:

$$H(s) = \frac{VU_z(s)}{I_z(s)}. \quad (18)$$

According to the method proposed in [12], a probe based on a combined electromagnetic acoustic transducer (EMAT) is placed above the medium in which the ultrasonic signal and the eddy current signal are simultaneously excited and received. These signals differ in time and space. The ECT signal is received almost immediately, while the typical time response for an ultrasonic signal is usually several mcs. Using time and amplitude selection, these signals are separated and processed individually, and then their characteristic parameters are used to solve the problem of determining the characteristics of iron ore and recognizing its mineralogical and technological varieties. Figure 4 shows a diagram of the time selection of received signals.

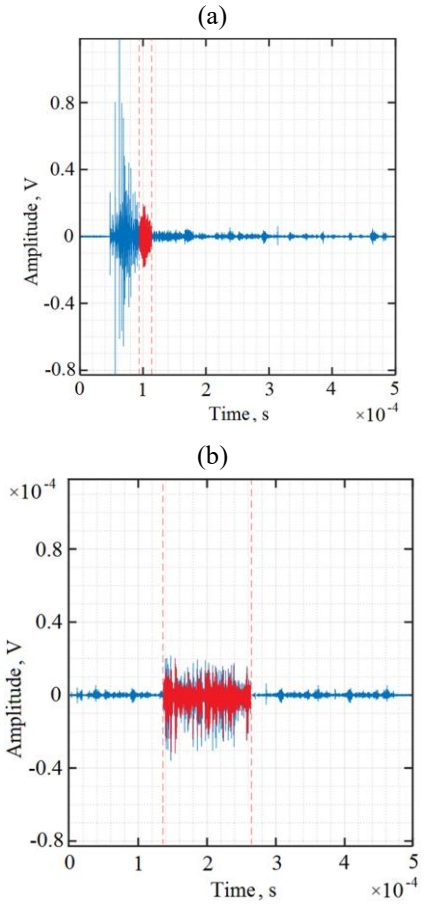

Figure 4. Temporal selection of received ECT and EMAT signals: (a) time response of the ECT signal, appearing almost instantly after excitation; the red interval marks the selected useful response; (b) time response of the ultrasonic (EMAT) signal, delayed by several microseconds; the red interval indicates the chosen analysis window

3. Results and discussion

The coil impedance of the eddy current sensor is a two-dimensional variable, so its real and imaginary parts can be represented on the impedance plane: the real part of the impedance is plotted on the *X*-axis, and the imaginary part is plotted on the *Y*-axis. In Figures 5-8 show graphs of the impedance plane when the distance of the sensor to the surface of the test medium changes, when the current frequency in the coil, the electrical conductivity, and the magnetic permeability of the test medium material located near the sensor change. The following sensor coil parameters were used in the modeling: r_0 = 5 mm, r_i = 2 mm, l_0 = 2 mm, n = 50.

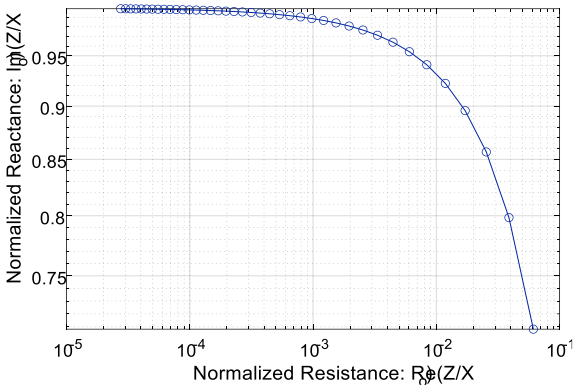

Figure 5. Plot of the impedance plane when changing the distance of the sensor to the surface of the medium under test from 0.5 to 20 mm, specific electrical conductivity of the medium σ = 50 S/m = 50·10⁻⁶ MS/m, magnetic permeability of the medium μr = 12, current frequency in the coil f = 220 kHz

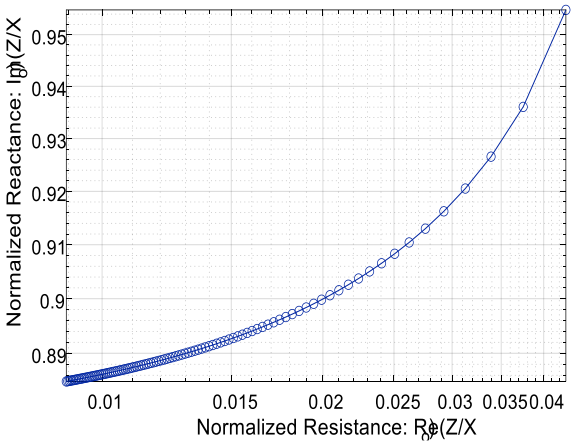

Figure 6. Plot of the impedance plane when the current frequency in the coil changes from 10 kHz to 1 MHz, the distance of the sensor to the surface of the medium under study is 2 mm, the specific electrical conductivity of the medium σ = 50 S/m = 50·10⁻⁶ MS/m, magnetic permeability of the medium μr = 12

Thus, the measured impedance values of the sensor coil characterize the properties of the medium, in particular the iron-bearing rock located next to it, but also require taking into account the distance between the coil and the medium.

The impedance (magnitude and phase) as a function of frequency is displayed (Fig. 9) using the impedance versus frequency measurement tool of the Powergui block. The Powergui block uses a method that uses a variable-step solver from Simulink® to determine the parameters of the circuit under study.

The impedance and the frequency at which its real and imaginary components are equal to each other are used as parameters determined as the result of eddy-current transformation.

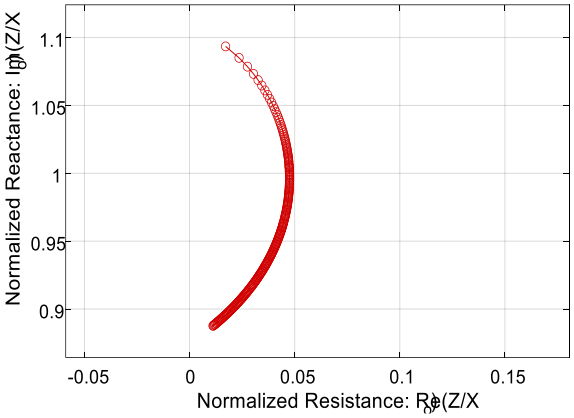

Figure 7. Plot of the impedance plane when the specific electrical conductivity of the medium changes σ from 5·10⁻⁶ to 500·10⁻⁶ MS/m, distance of the sensor to the surface of the medium under study 2 mm, magnetic permeability of the medium μr = 12, current frequency in the coil f = 220 kHz

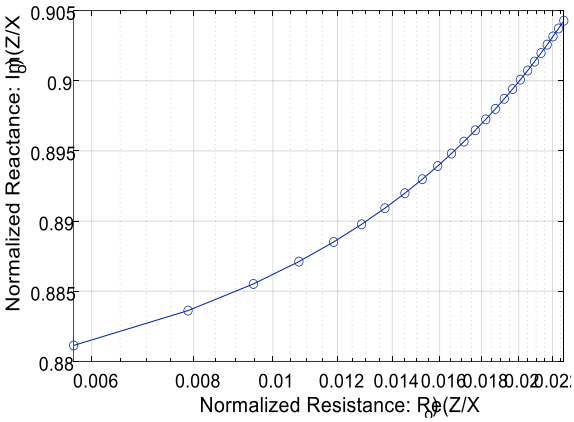

Figure 8. Plot of the impedance plane when the magnetic permeability of the medium changes μr from 1 to 25, distance of the sensor to the surface of the medium under study 2 mm, specific electrical conductivity of the medium σ = 50 S/m = 50·10⁻⁶ MS/m, current frequency in the coil f = 220 kHz

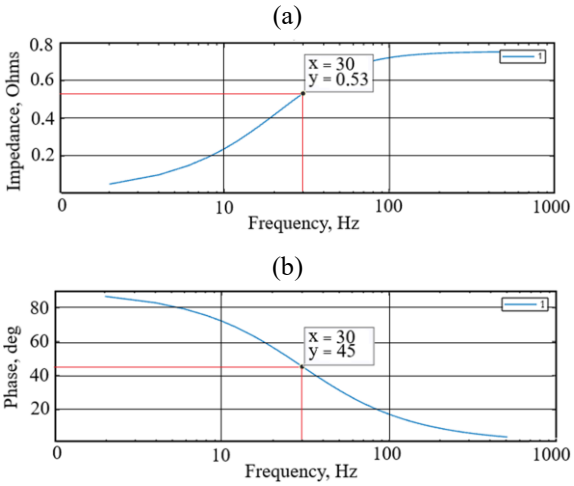

Figure 9. Impedance and phase as a function of the measurement signal frequency (R₀ = 0.75 Om; L₀ = 4·10⁻³ Hn): (a) frequency dependence of the impedance magnitude of the sensor coil, showing the characteristic growth with frequency; (b) frequency dependence of the impedance phase, illustrating the transition point where the real and imaginary components are equal

As follows from expressions (11) and (12), with a change in the current frequency $I(t)$ parameter values R_c and L_c change in opposite directions. So at a certain frequency w_m equality is achieved:

$$R_{cm} = jw_m L_{cm}\,, \tag{19}$$

where:

R_{cm}, L_{cm} – resistance and inductance of the measuring coil K_1, ensuring the fulfillment of equality (19) at the frequency w_m.

That is, the impedance of the measuring coil K_1 corresponds to the Expression:

$$Z_{cm} = R_{cm} + jw_m L_{cm}\,. \tag{20}$$

Measured impedance Z_{cm} characterizes the unique properties of the rock sample under study and, together with the frequency value w_m is a characteristic feature of the mineralogical type of rock.

To determine the electrical conductivity, magnetic permeability and mineralogical types of rock, a database is created that contains the relevant characteristic parameters of rock samples from the deposit under study. Measured values w_m correlate with exemplary ones w_{m0} and thus determine the desired parameter or type of rock. To improve the quality of recognition, it is advisable to combine the parameters w_m and Z_{cm} with other rock characteristics and use methods of intelligent classification of the obtained data set. To determine Equation (19), direct measurements are performed R_{cm}, L_{cm} and w using, for example, a phase-sensitive method (Fig. 8):

$$\varphi = arctg\left(\frac{X_{cm}}{R_{cm}}\right) = arctg\,(1) = 45°\,. \tag{21}$$

This result can also be obtained by approximating the measuring coil K_1 using a Foster network, i.e., a set of series-connected parallel RL sections (resistance, inductance) [24]. Our studies show that four such sections are sufficient to achieve an arbitrary approximation accuracy. To perform this approximation, the frequency of the signal supplied to the measuring coil K_1, changes in the specified range Δw. Next, an optimization computational procedure is performed to determine the following values of the parameters R and L of the Foster network that correspond to the measured impedance value Z_c. Next, an optimization computational procedure is performed to determine the following values of the parameters R and L of the Foster network, which correspond to the measured impedance of its components R_c and L_c.

This approach was used to determine the characteristics of iron ore and recognize its main types in a measuring channel based on combined electromagnetic acoustic transducers (EMATs) [12], [25], one of the possible embodiments of which is shown in Figure 10.

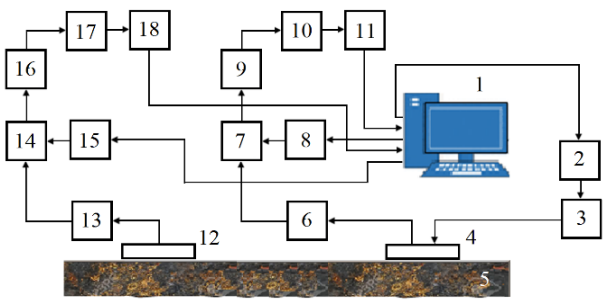

Figure 10. Structure of a combined measuring channel based on electromagnetic acoustic transducers

In accordance with the presented scheme (Fig. 10), computer *1* generates a task for the arbitrary function generator *2*. The signal generated in this unit is amplified using a power amplifier *3* before being fed to the electromagnetic converter *4*.

An acoustic electromagnetic transducer is used to generate elastic vibrations in the ferromagnetic conductive rocks of the rock mass. It is a distributed structure [12] consisting of a source of a constant magnetic field, a source of an alternating magnetic field, and a certain volume of the ferromagnetic component of the rock, where the processes of converting the energy of the electromagnetic field into the energy of elastic vibrations of the particles of the medium take place.

In the mode of excitation of elastic disturbances, the converter *4* realizes the conversion of electromagnetic signals into elastic vibrations of iron-containing rock due to the effects discussed in [12] (Lorentz force, magnetostrictive force, and magnetization force). At a certain point of the environment with coordinates x_k a constant magnetic field with intensity is formed $H^0(x_k)$ and variable (due to the influence of an electromagnetic pulse of a certain amplitude, duration and frequency) with a voltage $H^*(x_k, t)$ at a point in time t. In the region of existence of magnetic fields $H^*(x_k, t)$ and $H^0(x_k)$ deformations are formed in the medium. The energy in the zone of deformation formation is transmitted further by elastic waves. Thus, the acoustic transducer of electromagnetic type generates elastic vibrations directly in the zone of measuring the characteristics of iron-bearing rocks of the rock mass. Since there are no intermediate elements for transmitting the generated elastic vibrations to the medium, there are no errors in the procedure for measuring its characteristics caused by these factors.

In accordance with the above procedure, a pulsed eddy current is excited in the thickness of the skin layer of the medium under study under the influence of the electromagnetic field. As shown in Figures 5, 6, the characteristics of the medium affect the intensity and distribution of the pulsed eddy current, as well as the voltage on the electromagnetic transducer coil and its impedance.

The process of receiving the ultrasonic signal by the EMAP is directly opposite to the excitation process. When the ultrasonic wave propagates near the transducer receiving coil, the moving charged particles in the conductor generate a dynamic current under the action of the external magnetic displacement field. The dynamic current creates a dynamic magnetic field in and around the sample, and the receiving coil of the EMAP in this dynamic magnetic field generates a dynamically induced electromotive force, which is the generated signal in the coil.

Two variants of the measuring channel design are possible: a combined EMAP that simultaneously performs the functions of emitting and receiving the sensing signal, and two separate EMAPs (emitting and receiving). In the case of the first variant of this scheme, the signal received by the electromagnetic converter *4* is amplified by the preamplifier *6* and sent to the time selection unit *7*. According to the signal from the computer *1*, the selective pulse generating unit *8* generates a selective pulse, which, with the help of the selection unit *7*, "cuts out" the informative part of the received signal. This procedure is performed for both the eddy-current conversion process and the acoustic conversion process with respect to an ultrasonic wave that propagates and has traveled a certain distance in the medium under study (direct signal or backscattered). The received informative signal is filtered in the frequency filter *9*, finally amplified for further analysis in the unit *10*, converted to digital form in the analog-to-digital converter *11*, and fed to the computer *1*.

In the case of using the design of the measuring channel with two separate EMAPs, the electromagnetic transducer *4* in the receiving mode is used exclusively for processing the parameters of the eddy current conversion process. Receiving and pre-processing of ultrasonic signals that have traveled the appropriate distance in the test medium is performed by a separate circuit with a structure similar to the one considered: receiving electromagnetic transducer *12*, preamplifier *13*, selection unit *14*, selective pulse generator *15*, analog frequency filter *16*, main amplifier *17*, and analog-to-digital converter *18*.

To test the above approach, we used an experimental platform, the schematic of which is shown in Figure 9. A universal computer-controlled ultrasonic system RITEC RAM-5000 [26] was used to excite and process the EMAP signal, including limiting, multistage amplification, and bandpass filtering.

The used system provides pulsed ultrasonic measurements and resonant ultrasonic spectroscopy. The phase-sensitive superheterodyne receiver is capable of separating signals from noise, characterizing the materials under study by measuring attenuation, propagation speed, or resonant frequencies, covering a range of up to 40 MHz. The developed amplifier provides high power RF packet pulses up to 5 kW, RMS up to 7 MHz. A three-channel generator/receiver system is available with independent control of the packet width, frequency, delay, and phase for each output signal. Subunits of the ultrasonic granulometer "Pulsar" for the corresponding purpose were also used. A variant was investigated that, in order to increase the sensitivity of the method, involves the use of EMAT and ECT signals generated in different frequency ranges. In this case, a broadband sensing signal is formed [27].

$$S_M(t) = \sum_{k=1}^{N_s} S_k \sin\left(2\pi f_k t + \varnothing_k\right), \quad (22)$$

where:

$\varnothing_k$, f_k – phase and frequency is the k^{th} sinusoid;

N_s – the number of components.

The paper [28] considers an iterative method of fuzzy identification of mineralogical and technological varieties of iron ores based on the analysis of their properties in the vector space of features. The results of measuring the velocity and attenuation of longitudinal and transverse ultrasonic waves of the corresponding frequency are used as an information base for identifying mineralogical varieties of iron ores. based on which the acoustic quality coefficient of the rock sample is calculated, as well as a characteristic parameter determined by the dispersion and average intensity of the received ultrasonic signal that has traveled a certain distance in the studied medium [29], [30].

This method allows, by minimizing the weighted distances between the analyzed and reference values of the ultrasonic measurement results, to classify the sample under study with a certain degree of belonging to the main technological types of ores of the exploited deposit.

The use of the above-mentioned additional parameters Z_{cm} and w_m, determined based on the results of eddy current conversion of the probing electromagnetic signal, for the recogni-

tion of mineralogical varieties of iron ores allows improving the quality of the results obtained compared to exclusively ultrasonic measurements. In particular, the confidence probability of recognizing the main mineralogical and technological varieties of iron ore in the studied deposit increases to 94.5%.

4. Conclusions

Eddy current testing has become one of the most common methods for measuring the characteristics of electrically conductive materials and structures in various industrial sectors, such as infrastructure, automotive, metallurgical production, and chemical engineering. Significant progress has been made in determining the geometry, electromagnetic properties, and defects of metal structures based on electromagnetic principles. Importantly, eddy current measurements do not require the test object to be in direct contact with the test equipment.

Variations in the electrical conductivity and magnetic permeability of iron ore, associated with its specific physical and chemical properties and textural and structural characteristics, lead to changes in the conditions of formation and flow of eddy currents, which is reflected in the phase, amplitude, and spectral composition of the signal in the receiving circuit of the eddy current sensor.

The transformer model of the eddy current sensor accurately reflects the processes occurring within it. When modeling the dependencies of the eddy current sensor parameters on the characteristics of the environment under study, its model in the form of two coils with air cores located one above the other at a certain distance was used.

The measured impedance values of the sensor's measuring coil characterize the properties of the environment, in particular the iron-bearing rock located next to it. The dependencies obtained as a result of modeling eddy current conversion are used in the development of a method for non-contact non-destructive measurement of iron ore characteristics.

The direction of further research is to justify the technology of using a combined electromagnetic acoustic and eddy current conversion method for recognizing mineralogical and technological varieties of iron ore during its extraction and processing.

Author contributions

Conceptualization: VM, NM; Data curation: TO, SH; Formal analysis: TO, SH; Funding acquisition: NM; Investigation: VM, NM, TO, SH; Methodology: VM, NM; Project administration: NM; Resources: TO, SH; Software: SH; Supervision: VM, SH; Validation: NM, TO; Visualization: SH; Writing – original draft: VM, NM; Writing – review & editing: VM, NM, TO, SH. All authors have read and agreed to the published version of the manuscript.

Funding

This research was funded by the Alexander von Humboldt Foundation.

Conflicts of interest

The authors declare no conflict of interest.

Data availability statement

The original contributions presented in the study are included in the article, further inquiries can be directed to the corresponding author.

References

[1] Sophian, A., Tian, G., & Fan, M. (2017). Pulsed eddy current non-destructive testing and evaluation: A review. *Chinese Journal of Mechanical Engineering*, *30*, 500-514. https://doi.org/10.1007/s10033-017-0122-4

[2] Ribeiro, A., Ramos, H.G., & Couto, A.J. (2012). Liftoff insensitive thickness measurement of aluminium plates using harmonic eddy current excitation and a GMR sensor. *Measurement*, *45*(9), 2246-2253. https://doi.org/10.1016/j.measurement.2012.04.025

[3] Harms, J., & Kern, T.A. (2021). Theory and modeling of eddy current type inductive conductivity sensors. *Engineering Proceedings*, *6*(1), 37. https://doi.org/10.3390/I3S2021Dresden-10103

[4] Moulder, J.C., Uzal, E., & Rose, J.H. (1992). Thickness and conductivity of metallic layers from eddy current measurements. *Review of Scientific Instruments*, *63*(6), 3455-3465. https://doi.org/10.1063/1.1143749

[5] Lakhdari, A.E., Cheriet, A., & El-Ghoul, I.N. (2019). Skin effect based technique in eddy current non-destructive testing for thickness measurement of conductive material. *IET Circuits, Devices & Systems*, *13*(2), 255-259. https://doi.org/10.1049/iet-smt.2018.5322

[6] Rodrigues, N., Rosado, L., & Ramos, P.M. (2016). Portable embedded system for contactless measurement of material conductivity. *Proceedings of the International Symposium and Workshop on ADC Modelling and Testing*, 102-106. https://doi.org/10.13140/RG.2.2.23860.17289

[7] Glenn, S.S. (2014). A simple derivation for the skin effect in a round wire. *European Journal of Physics*, *35*(2), 025002. https://doi.org/10.1088/0143-0807/35/2/025002

[8] Gruber, G., Schweighofer, B., Berger, M., Leitner, T., Kloesch, G., & Wegleiter, H. (2024). Eddy current position measurement in harsh environments: A temperature compensation and calibration approach. *Sensors*, *24*(5), 1483. https://doi.org/10.3390/s24051483

[9] Tagger, S., Neumayer, M., & Gruber, G., Wegleiter, H. (2022). Metrological analysis of a contactless inductive position measurement system. *Proceedings of the 2022 IEEE Sensors Applications Symposium (SAS)*, 1-6. https://doi.org/10.1109/SAS54819.2022.9881383

[10] Wang, H., Liu, Y., Li, W., & Feng, Z. (2014). Design of ultrastable and high-resolution eddy-current displacement sensor system. *Proceedings of the IECON 2014 – 40th Annual Conference of the IEEE Industrial Electronics Society*, 2333-2339. https://doi.org/10.1109/IECON.2014.7048828

[11] Zablocki, C.J. (1966). Electrical properties of some iron formations and adjacent rocks in the Lake Superior region. *Mining Geophysics*, *1*.

[12] Morkun, V.S., Morkun, N.V., Hryshchenko, S.M., Gaponenko, A.A., Gaponenko, I.A., & Bobrov, E.Y. (2023). Modeling of an electromagnetic acoustic transducer. *Mining Bulletin*, *111*, 88-95. https://doi.org/10.31721/2306-5435-2023-1-111-88-95

[13] Morkun, V., Morkun, N., & Pikilnyak, A. (2014). Simulation of Lamb waves propagation on the plate which contacts with gas containing iron or pulp in Waveform Revealer toolbox. *Metallurgical and Mining Industry*, *6*(5), 15-18.

[14] Morkun, V., & Morkun, N. (2018). Estimation of the crushed ore particles density in the pulp flow based on the dynamic effects of high-energy ultrasound. *Archives of Acoustics*, *43*(1), 61-67. https://doi.org/10.24425/118080

[15] Azaryan, A.A., Batareyev, O.S., Karamanits, F.I., Kolosov, V.O., & Morkun, V.S. (2018). Ways to reduce ore losses and dilution in iron ore underground mining in Kryvbass. *Science and Innovation*, *14*(4), 17-24. https://doi.org/10.15407/scine14.03.017

[16] Stawicki, O., Ahlbrink, R., & Schröer, K. (2009). Shallow internal corrosion sensor technology for heavy pipe wall inspection. *Proceedings of the PPSA Seminar*, *18*, 1-7.

[17] Libby, H.L. (1971). *Introduction to electromagnetic nondestructive test methods*. New York, United States: Wiley-Interscience, 378 p.

[18] Krahenbuhl, L., & Muller, D. (1993). Thin layers in electrical engineering: Example of shell models in analysing eddy-currents by boundary and finite element methods. *IEEE Transactions on Magnetics*, *29*(2), 1450-1455. https://doi.org/10.1109/20.250676

[19] Placko, D., & Dufour, I. (1992). Eddy current sensors for nondestructive inspection of graphite composite materials. *Proceedings of the IEEE Industry Applications Society Conference*, 1676-1682. https://doi.org/10.1109/IAS.1992.244235

[20] Xu, P., Huang, S., & Zhao, W. (2010). Differential eddy current testing sensor composed of double gradient winding coils for crack detection. *Proceedings of the IEEE Sensors Applications Symposium*, 59-63. https://doi.org/10.1109/SAS.2010.5439405

[21] García-Martín, J., Gómez-Gil, J., & Vázquez-Sánchez, E. (2011). Non-destructive techniques based on eddy current testing. *Sensors*, *11*, 2525-2565. https://doi.org/10.3390/s110302525

[22] Brinker, K. (2023). Eddy current scenario simulator. *MATLAB Central File Exchange. MATLAB Help Center*. Retrived from:

https://www.mathworks.com/matlabcentral/fileexchange/108954-eddy-current-scenario-simulator
[23] Simscape. (2024). *Model and simulate multidomain physical systems*. Retrived from: https://www.mathworks.com/products/simscape.html
[24] Thompson, S.C. & Warren, D.M. (2017). Analog circuit model for loudspeakers including eddy current behavior and suitable for time domain simulation. *AES Convention*, *9826*, 1-12.
[25] Guo, W., Gao, B., Yun, Tian G., & Si, D. (2020). Physic perspective fusion of electromagnetic acoustic transducer and pulsed eddy current testing in non-destructive testing system. *Philosophical Transactions of the Royal Society A: Mathematical, Physical and Engineering Sciences*, *378*, 20190608. https://doi.org/10.1098/rsta.2019.0608
[26] *RITEC RAM System Versatile Ultrasonic System for Pulsed Ultrasonics and Resonant Ultrasound Spectroscopy*. (2024). Available at: http://www.ritecinc.com/ramspecs.pdf
[27] Ali, K.B., Abdalla, A.N., Rifai, D., & Faraj, M.A. (2017). Review on system development in eddy current testing and technique for defect classification and characterization. *IET Circuits, Devices & Systems*, *11*(4), 338-351. https://doi.org/10.1049/iet-cds.2016.0327
[28] Morkun, V., Morkun, N., Fischerauer, G., Tron, V., Haponenko, A., & Bobrov, Y. (2024). Identification of mineralogical ore varieties using ultrasonic measurement results. *Mining of Mineral Deposits*, *18*(3), 1-8. https://doi.org/10.33271/mining18.03.001
[29] Morkun, V.S., Morkun, N.V., & Tron, V.V. (2017). Automatic control of the ore suspension solid phase parameters using high-energy ultrasound. *Radio Electronics, Computer Science, Control*, *3*, 175-182. https://doi.org/10.15588/1607-3274-2017-3-19
[30] Morkun, V., Morkun, N., Tron, V., Hryshchenko, S., Serdiuk, O., & Dotsenko, I. (2019). Basic regularities of assessing ore pulp parameters in gravity settling of solid phase particles based on ultrasonic measurements. *Archives of Acoustics*, *44*(1), 161-167. https://doi.org/10.24425/aoa.2019.126362

Використання вихрострумового перетворення для реалізації комбінованого електромагнітного методу визначення характеристик залізної руди

В. Моркун, Н. Моркун, Т. Олійник, С. Грищенко

Мета. Визначення характеристичних параметрів електромагнітного вихрострумового перетворення для розпізнавання мінералогічних різновидів залізної руди.

Методика. У роботі використані методи аналізу вітчизняного та закордонного досвіду, а також методи математичного аналізу і комп'ютерного моделювання для визначення впливу специфічних фізико-хімічних властивостей та текстурно-структурних особливостей залізовмісних гірських порід на характеристики вихрострумового перетворення зондуючого електромагнітного сигналу. Для визначення частоти зондуючого сигналу, на якій дорівнюють одна одній дійсна та уявна складові імпедансу вимірювальної котушки датчика, здійснюється її апроксимація за допомогою мережі Фостера.

Результати. Варіації електропровідності та магнітної проникності залізної руди, пов'язані з її мінералогічним складом і фізичною структурою, призводять до змін умов формування й перебігу вихрових струмів, що відбивається на фазі, амплітуді та спектральному складі сигналу в приймальному контурі вихреструмового датчика. Виміряні значення імпедансу вимірювальної котушки датчика характеризують унікальні властивості досліджуваного зразка гірської породи і разом із значенням частоти зондуючого електромагнітного сигналу є характеристичною ознакою мінералогічного різновиду гірської породи.

Наукова новизна. Вперше встановлено, що визначені за результатами вихрострумового перетворення у феромагнітному середовищі зондуючого електромагнітного сигналу змінюваної частоти значення дійсної та уявної складових імпедансу вимірювальної котушки і частоти, на якій вони дорівнюють одна одній, відповідають унікальним фізико-хімічним властивостям мінералогічних різновидів досліджуваної залізовмісної гірської породи і є ефективними характеристичними ознаками для їх розпізнавання.

Практична значимість. Отримані за результатами моделювання вихрострумового перетворення залежності використані при реалізації методу безконтактного неруйнівного вимірювання характеристик залізної руди і розпізнавання її мінералогічних різновидів. Результати випробувань та практичної апробації запропонованого методу свідчать про його високу ефективність, що дозволяє рекомендувати розроблені науково-технічні рішення для широкого промислового застосування на гірничодобувних підприємствах.

Ключові слова: *руда, різновиди, розпізнавання, електромагнітне перетворення, характеристики, вимірювання, моделювання*

Publisher's note

All claims expressed in this manuscript are solely those of the authors and do not necessarily represent those of their affiliated organizations, or those of the publisher, the editors and the reviewers.